

MEMS-based Micro Instruments for In-Situ Planetary Exploration

T. George^a, E. Urgiles^a, R. Toda^a, J.Z. Wilcox^a, S. Douglas^a, C-S. Lee^a, K. Son^a, D. Miller^a,
N. Myung^a, L. Madsen^b, G. Leskowitz^b, R. El-Gammal^b, and D. Weitekamp^b

^aJet Propulsion Laboratory,

^bCalifornia Institute of Technology, Pasadena, CA 91109

Mailstop: 302-306, 4800 Oak Grove Drive, Pasadena, CA 91011

Email: Thomas.George@jpl.nasa.gov

ABSTRACT

NASA's planetary exploration strategy is primarily targeted to the detection of extant or extinct signs of life. Thus, the agency is moving towards more in-situ landed missions as evidenced by the recent, successful demonstration of twin Mars Exploration Rovers. Also, future robotic exploration platforms are expected to evolve towards sophisticated analytical laboratories composed of multi-instrument suites. MEMS technology is very attractive for in-situ planetary exploration because of the promise of a diverse and capable set of advanced, low mass and low-power devices and instruments. At JPL, we are exploiting this diversity of MEMS for the development of a new class of miniaturized instruments for planetary exploration. In particular, two examples of this approach are the development of an Electron Luminescence X-ray Spectrometer (ELXS), and a Force-Detected Nuclear Magnetic Resonance (FDNMR) Spectrometer. The ELXS is a compact (< 1 kg) electron-beam based microinstrument that can determine the chemical composition of samples in air via electron-excited x-ray fluorescence and cathodoluminescence. The enabling technology is a 200-nm-thick, MEMS-fabricated silicon nitride membrane that encapsulates the evacuated electron column while yet being thin enough to allow electron transmission into the ambient atmosphere. The MEMS FDNMR spectrometer, at 2-mm diameter, will be the smallest NMR spectrometer in the world. The significant innovation in this technology is the ability to immerse the sample in a homogenous, uniform magnetic field required for high-resolution NMR spectroscopy. The NMR signal is detected using the principle of modulated dipole-dipole interaction between the sample's nuclear magnetic moment and a 60-micron-diameter detector magnet. Finally, the future development path for both of these technologies, culminating ultimately in infusion into space missions, is discussed.

Keywords: MEMS, in-situ, planetary exploration, micro-instrument, NASA, JPL, x-ray fluorescence, cathodoluminescence, ELXS, NMR, FDNMR, life detection.

INTRODUCTION

NASA In-Situ Mission background

Robotic planetary exploration has a rich history at NASA starting from its origins with the successful Explorer mission¹ launched in 1958, and which led to the discovery of the Van Allen Belts that cover the earth. Since then, several robotic exploration missions have been successfully accomplished by many space organizations around the world. These explorations have occurred in either of three modes: fly by missions, planetary orbiting missions, and landed, in-situ missions. In general, the order of these modes also represents the chronological order in which planetary exploration missions have been conducted, with fly by missions providing the initial survey information, followed by more detailed information being provided by orbiting missions and ultimately by landed, in-situ missions. Although the search for signatures of extra-terrestrial life has always been a key objective for NASA's planetary exploration missions, during the last decade this "astrobiology" objective has gained ascendance as a primary goal for these missions. In fact, NASA's future planetary exploration strategy is succinctly described by one of its vision statements, which is "To find life beyond".

Case for sophisticated instruments

The search for life is complicated by the fact that there does not exist a single, conclusive measurement for signatures of extinct life on a planet. There is however, general agreement within the scientific community that the astrobiology exploration strategy should be based on the following two principles:

1. The astrobiological investigation has to be conducted over several length scales, from the macroscopic, planetary scale (few thousand kilometers) to the microscopic, mineral grain scale (few micrometers). A well-known, macroscopic biogenic effect is the presence of oxygen in our earth atmosphere. At the other spatial scale extreme, bacteria are known to modify the microstructural chemical composition of rocks and minerals.
2. Barring the return of planetary specimens to terrestrial laboratories for analysis, a sophisticated, multi-instrument suite will be necessary for in-situ astrobiology investigations. It is hoped this instrument suite will gather individually distinct and yet complementary sets of evidence to support the powerful conclusion on whether life existed on another planet. Even for the case of sample return missions, a multi-instrument suite would be desirable for the selection of appropriate samples.

Goal number seven of NASA's Astrobiology Roadmap² is to "Determine how to recognize the signature of life on other worlds." In particular, it states that "based upon our experiences here on Earth, we must learn to recognize fossil structures and chemical traces of extinct life that may be present in extraterrestrial rocks or other samples". Life as we know it requires the following basic ingredients: Liquid water, a large pool of organic compounds and an energy source driving the synthesis of biologically relevant, complex molecules. Thus, a "follow the water" strategy has been adopted as a key thrust for Astrobiology investigations. From, a planetary investigation perspective, both Titan and Mars are targets of high astrobiological interest for different reasons. In the case of Titan, with its substantial inventory of reduced carbon but extraordinarily low surface temperature, life is not expected to have formed. However, surface geologic processes, including impacts and cryovolcanism, would have provided brief periods in restricted places where organics could have been exposed to liquid water. Mars on the other hand, had an early history in which liquid water was present on or near the surface, during which time life could have formed. Whether life exists today in the deep crust of Mars (by analogy with endolithic organisms recently discovered on Earth) is an open issue. A key goal of the Mars exploration program is to detect and analyze biogenically modified rocks and minerals, as well as extract sub-surface organic phases that have been protected from the extremely oxidizing surface soil layer. Although organic bio-markers provide the strongest evidence of extinct life, the effects of environmental degradation could potentially destroy these signatures in a few tens of millions of years.³ Therefore Martian in-situ exploration missions will also necessarily have instruments targeted to the study of minerals and fossils found in sedimentary deposits from paleo-lake or ocean beds. If the origin of life on Mars did follow a similar path as on earth, then, as observed on earth, small life forms such as bacteria could have modified the composition and structure of rocks and minerals.

To date, NASA and other space agencies have flown several different types of instruments. Most of these instruments fall into the general class of optical imagers and spectrometers. Although important in their own right, these instruments are a limited set in that they provide only part of the data set required for conclusive determination of the signatures of extinct life. In addition to optical instruments, previous missions have also carried x-ray fluorescence instruments, gas chromatographs, mass spectrometers and some wet chemistry instrumentation.⁴ In order to take on the difficult challenge of determining signatures of extinct life in-situ, this limited instrument set will have to be expanded considerably to include other, complementary measurements. It is envisioned that future in-situ exploration laboratory platforms will also have an integral planetary specimen acquisition and processing station. Therefore, in principle, it will be possible to derive the complementary data sets by transporting sequentially, using microfluidics or otherwise, the same planetary specimen to each of the various instruments within the suite.

Planetary instrument requirements

There are a number of important considerations to keep in mind for the development of instruments for robotic planetary exploration. Since, in nearly every case, it is impossible to send a "repair man" to fix problems that arise during the mission, these instruments have to be inherently robust and operate reliably for the entire duration of the mission. Shock and vibration loads during launch and deployment can be considerable (many times the gravitational acceleration). Next, depending on the level of insulation and shielding, the instrument could be subjected to extremes in temperature and pressure, from 470°C and several atmospheres on Venus,⁵ to near vacuum and -170°C on Europa,⁶ a moon of Jupiter. The effect of radiation could be a major consideration. For instance on Europa, also considered to be a good astrobiology

mission target, landed spacecraft would be subjected to an estimated 7 MRad of radiation. Finally, the atmospheric ambient itself could be an extremely harsh environment. Venus, for instance, has an atmosphere containing sulfuric acid. Thus, both the planet and the site on the planet can determine the environmental conditions under which each instrument suite would have to operate. It is a remarkable fact therefore, that many previous in-situ planetary exploration missions have succeeded despite the unforgiving nature of the space environment.

Diversity of MEMS

Micro Electro Mechanical Systems (MEMS) technology promises exactly what space missions need, which are highly capable systems with low mass and power consumption. MEMS comprise a broad range of miniaturized sensing and actuation technologies that could be utilized in practically every aspect of the spacecraft and instrument payload. To date, MEMS-based accelerometers, gyroscopes, strain, pressure, and temperature sensors have found application in aerospace systems. However, the role of MEMS can be expanded greatly in future space missions. For instance, MEMS technologies can be used in the sample acquisition and transport system for the multi-instrument suite. More important still is the role of MEMS in enabling a new class of sophisticated instruments. At the Jet Propulsion Laboratory (JPL) we have utilized MEMS techniques successfully for the development of two such novel, astrobiology instruments namely, the Electron Luminescence X-ray Spectrometer (ELXS) and the Force-Detected Nuclear Magnetic Resonance (FDNMR) spectrometer described below.

Rationale for the ELXS and FDNMR

The ELXS instrument is a unique MEMS-based instrument that extends the capability of current x-ray fluorescence (XRF) instruments by the addition of a simultaneous electron-beam excited optical luminescence or cathodoluminescence measurement. XRF analysis is a standard technique and has been used on every landed planetary mission for the determination of elemental compositions of rocks and soils. With the additional cathodoluminescence capability, the ELXS can be a powerful tool for astrobiology investigations. It is well known that some biogenic materials such as mollusk shells exhibit cathodoluminescence.⁷ Thus, cathodoluminescence could be used as a technique to differentiate between naturally occurring carbonate minerals and those of biogenic origin.

The ELXS development traces back its origins to a novel concept for a “Miniature Electron Microscope without Vacuum Pumps” proposed by T. George.⁸ This concept described the means for obtaining electron beam-excited x-ray fluorescence in air from samples by using miniature electron sources encapsulated by electron-transmissive membranes. This concept was later expanded to include cathodoluminescence.⁹ Electron-beam analysis in non-vacuum ambients has been proposed before.^{10,11} However, as opposed to the ELXS, these techniques were aimed at developing scanning electron microscopy imaging techniques at atmospheric pressure and low pressure (7 torr). The ELXS is being developed as a potential successor for the successful Alpha Particle X-ray Spectrometer (APXS)¹² that has been flown several times on Mars exploration missions.¹³ The ELXS excels in rapid elemental analysis in comparison to competing planetary x-ray fluorescence techniques (Table 1). This is because the ELXS, with modest beam currents, produces a high flux of electrons for a high XRF yield, leading consequently to rapid spectrum acquisition and low power consumption. Also, by having a focused electron beam, the ELXS is able to achieve higher spatial resolution.

Table 1: Comparison of ELXS properties with competing x-ray fluorescence instruments

Features	ELXS	X-ray based XRF ¹⁴	APXS ^{12,13}
Excitation particles	Electrons	X-ray photons	α-particles
Particle flux	6x10 ¹³ /s (10μA)	Primary electron beam: 0.3mA; X-ray photon yield: 2x10 ¹² /s	2x10 ⁹ /s (30mCi)
Power consumption	5 W (peak operation)	13 W	1 W
XRF yield (photons/second)	> 2x10⁴	10 ² to 10 ³	~ 1
Spectrum acquisition time ¹	< 10 seconds	5 minutes	0.5 hour
Energy per acquired spectrum	< 50 J	5,000 J	500 J
Spatial resolution	Variable (<mm² - cm²)	~4 cm ² (at 2 cm working distance)	~ 11 cm ²

Nuclear magnetic resonance (NMR) is the primary spectroscopic technique used by chemists for elucidating the molecular structure and dynamics of organic compounds in either liquid or solid states. However, an NMR instrument has never been flown primarily because of mass and power constraints. The conventional NMR spectrometer used in laboratories is a room-sized instrument that employs massive superconducting magnets. The reason that NMR is of interest for astrobiology investigations is because its particular strength, unmatched by other, competing techniques, is in the detection and distinction of water in either the physisorbed or chemisorbed states. A miniaturized NMR instrument will therefore be an important addition to the next generation of sophisticated astrobiology instruments, for the detection and characterization of water and organics. At JPL, we are developing the world's smallest (2 mm diameter), high-resolution FDNMR spectrometer for planetary astrobiological investigations.¹⁵ The MEMS FDNMR spectrometer concept was invented by the Weitekamp group at Caltech¹⁶ and is designed to be able to characterize 60-micron-sized specimens with a detection-limit of between 10^{11} - 10^{12} nuclear spins at room temperature. In practical terms, this detection ability translates to between 0.2-2 picomoles of glycine (H_2NCH_2COOH). It is envisaged that the FDNMR spectrometer will be one of the miniature instruments integrated within the multi-instrument suite with an integrated microfluidic sample transport system.

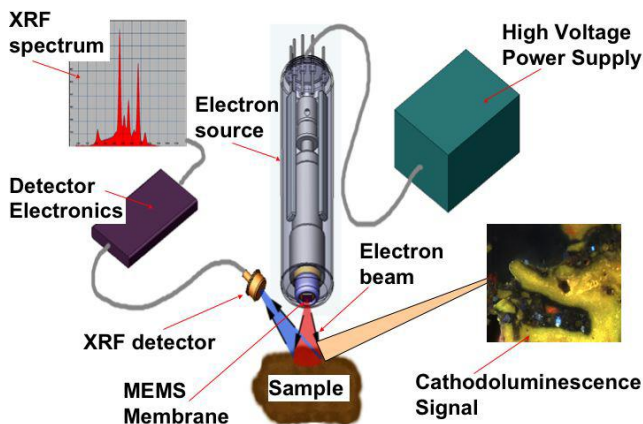


Figure 1: Schematic diagram showing the main components and the operation of the ELXS instrument. A high energy (20 keV) electron beam is generated within the vacuum-encapsulated electron source. The beam traverses the MEMS-fabricated, SiN encapsulation membrane and strikes the sample generating x-ray fluorescence and optical luminescence (cathodoluminescence).

ELECTRON LUMINESCENCE X-RAY SPECTROMETER

Design and Construction

The MEMS-enabled ELXS consists of the following components as shown in Figure 1. A commercially available, miniature electron source is vacuum-encapsulated using a MEMS-fabricated SiN membrane (Fig. 2). The electron source is capable of producing 20 keV electrons that traverse the SiN membrane and excite both x-ray fluorescence and optical luminescence from the target sample present in the ambient atmosphere. The x-ray fluorescence is detected using a silicon P-I-N diode detector that converts the x-ray photons into current pulses of electron-hole pairs. The height of the current pulse corresponds to the energy of the detected x-ray photon. A downstream multichannel analyzer “bins” the current pulses into the appropriate x-ray energy channels, generating the XRF spectrum shown in the figure. The XRF peaks are characteristic emissions from the various elements present in the sample. The elemental composition of the sample can then be determined by analysis of the XRF spectrum. Simultaneously, with the XRF emission, the sample may also emit cathodoluminescence (CL). Carbonate minerals found within organisms such as mollusks, or cyanobacteria, also exhibit CL due to the

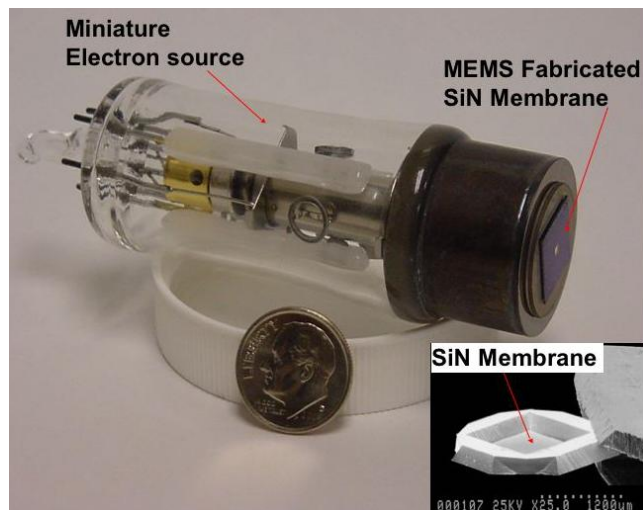


Figure 2. Vacuum encapsulated miniature electron source. The encapsulation membrane is anodically bonded to the electron source. Inset shows the MEMS-fabricated 200-nm-thick SiN membrane.

incorporation of trace amounts of Mn. The fluorescence in the visible/near infrared is primarily due to the presence of Mn^{2+} substituting for Ca^{2+} in the carbonate crystal structure. CL spectra have also been used to determine the presence of other activating ions such as trivalent rare earth elements and transition elements (e.g., Fe^{3+} , Cr^{3+}) that are well below the detection limit of conventional x-ray fluorescence analyses (e.g., 10's to 100's of parts per million). In addition, CL often illuminates the internal structures and outlines of fossils that may be invisible in reflected light.

ELXS characterization was conducted by mounting the miniature electron source within a vacuum pumped “environmental” chamber (Fig. 3) capable of adjusting the composition and pressure of the gaseous ambient in order to simulate planetary atmospheric conditions. A solid-state, PIN diode, x-ray detector was mounted within the environmental chamber to detect the electron-beam induced x-ray fluorescence. Although visible light cathodoluminescence was observed using the ELXS setup in air, detailed measurements were obtained separately using a scanning electron microscope (SEM) model LEO Supra 50 VP equipped with a Gatan Mono CL3 unit.

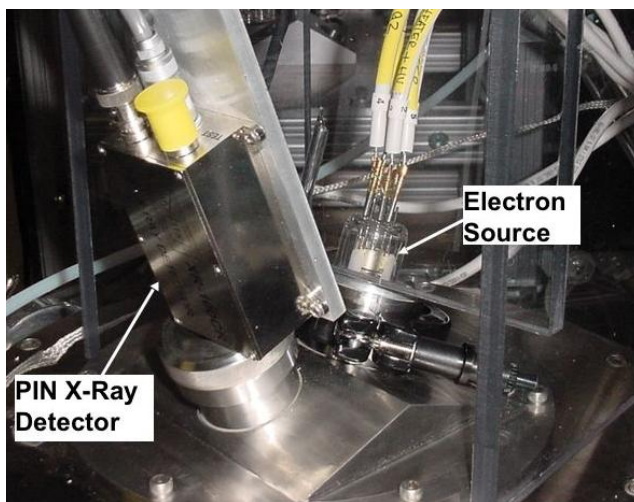


Figure 3. View of the top flange of the environmental chamber showing the electron source and the solid-state, PIN diode, x-ray fluorescence detector. The composition and pressure of gaseous mixtures within the environmental chamber can be adjusted to simulate planetary atmospheric conditions.

Testing and Characterization

The MEMS-fabricated SiN vacuum-encapsulation membrane is the core enabling technology for the ELXS instrument. Therefore a number of tests were conducted in order to test the properties of the SiN membrane. These included:

1. **Vibration and Shock testing:** The membrane successfully passed vibration and shock tests developed for instrument payloads for Mars landed missions. This mechanical robustness is to be expected because although the membrane is fragile and can break during handling, once integrated, the self-forces generated are very small (100nN for 10g acceleration).
2. **Gas Leak rate:** Vacuum degradation is a concern for the ELXS due to gas diffusion through the membrane. The leak rate of the membrane has been measured using an MKS Vac-Check 100 residual gas analyzer in the Helium leak check mode. A 500nm thick, 1mm square membrane exhibited no appreciable change to the background leak rate of 1×10^{-13} Torr-liters/sec.
3. **Electron transmission properties:** The electron beam undergoes both elastic and inelastic scattering during transmission through the SiN membrane and the surrounding atmosphere. Elastic scattering follows the Rutherford collision model and causes the electron beam to diverge without changing the beam energy. Inelastic scattering on the other hand cause the beam to lose energy by various loss mechanisms including photon generation and heating. Both of these effects influence the ultimate XRF and CL yield. The elastic scattering effect is more pronounced because it determines the ultimate spatial resolution of the ELXS. A beam divergence measurement experiment was conducted under well-controlled conditions in an SEM (Fig. 4). The SiN membrane was mounted in a specially constructed fixture underneath the objective lens. The divergence of the electron beam exiting the SiN membrane was measured by analyzing the XRF yield from a “knife-edge” sample translated horizontally across the irradiated spot. The knife-edge edge sample consisted of a GaAs wafer, partially coated with a thin film of Cu, having a well-defined edge. The GaAs XRF counts were measured as a function of sample translation. The results are shown in Figure 4 as a function of the membrane-to-sample distance. The full width at half maximum (spatial resolution) for the irradiated spot corresponds roughly to half the membrane-to-sample distance. Also, the XRF intensity is attenuated with increasing membrane-to-sample distance. This attenuation could be due to both, a decrease in electron beam intensity, as well as a decrease in the solid angle subtended by the XRF detector at the sample.

Detailed characterization of the ELXS was conducted using a number of standard samples with well-known compositions. The characterization experiments fell into two categories:

1. XRF characterization: The x-ray fluorescence excitation capability of the ELXS was characterized using a set of standard samples, which included metals, compounds and minerals. The characterization was performed within the environmental chamber, in which the ambient pressure was varied from earth atmospheric pressure down to vacuum. Two experiments are worthy of note and pertain to the ultimate in-situ planetary exploration application on Mars.¹⁷ The first was an experiment to determine whether the ELXS could potentially identify different mineral types within a Martian atmosphere ambient (8 Torr). The second experiment was to determine the attenuation of the XRF signal with increase in the surrounding atmospheric pressure.

Mineral identification: For the first, mineral identification experiment, several USGS standard powder samples were chosen. These mineral samples had different chemical compositions and were representative of various rock forming environments. The following samples were studied:

- BCR-2: Basalt, Columbia River, mined from the Bridal Veil Flow Quarry in Portland, Oregon
- MAG-1: Marine Sediment, a fine grained gray-brown clayey mud with low carbonate content from the Wilkinson Basin off the Gulf of Maine
- QLO-1: Quartz Latite collected in Lake County, Oregon from a lava flow dating back to probably the late Miocene or early Pliocene periods
- SDO-1: Reference Shale sample collected from the Huron Member of the Ohio Shale near Morehead, Kentucky.

Figure 5 contains the XRF spectra obtained from these four samples. The Basalt XRF spectrum shows a distinctive Ca peak, while the Marine Mud sample has a prominent Cl peak, the Shale has a significant S peak, and, as expected, the Quartz exhibits the most intense Si peak. The calculated values of the elemental composition were compared against the USGS certified compositions for these minerals. The compositional variation in all cases was found to be below 5% of the total analyzed concentration.

Effect of ambient pressure on XRF Attenuation: The effect of ambient pressure on the attenuation of the ELXS-generated XRF signal was also characterized for a range of pressures (Fig. 6). As discussed above, the attenuation could be due to several effects, including: electron beam scattering and x-ray fluorescence absorption. Although there is a monotonic decrease in the XRF signal with increase in ambient pressure, two distinct pressure regimes were identified.¹⁷ Weakly attenuated XRF spectra were obtained for the ambient pressure regime between 0-100 Torr, while above 100 Torr the XRF spectra were strongly attenuated. Pronounced attenuation was observed for low-energy x-rays emitted by the lower atomic number elements. Thus, strong XRF attenuation affects compositional measurements in two ways, the acquisition

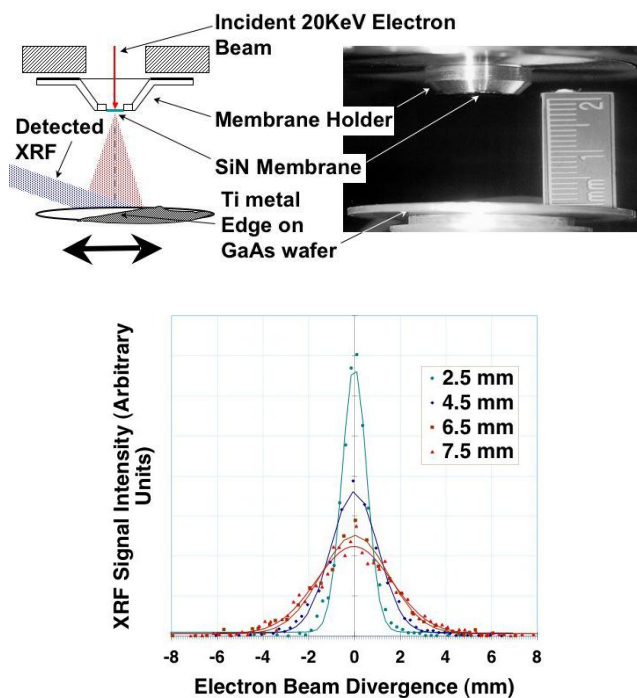


Figure 4. Electron beam divergence experiment conducted in a scanning electron microscope. The SiN membrane was placed in a specially constructed holder placed beneath the objective lens. A GaAs wafer coated partially with a Cu thin film with a well defined edge was then translated across the divergent electron beam exiting the membrane. X-ray fluorescence from the GaAs was measured as a function of the horizontal translation of the wafer. The resulting beam divergence plots are shown above with the full width at half maximum of beam divergence being roughly half the distance between the membrane and the sample. Also, as expected, the XRF intensity decreases with increasing membrane-to-sample distance.

time for XRF spectra increases, and erroneous elemental composition values may be obtained due to the enhanced low-energy x-ray attenuation.

2. Cathodoluminescence characterization:

Cathodoluminescence experiments were conducted in an SEM as described above. Unfortunately, our results were not conclusive in that a definite optical signature or set of signatures for the presence of biogenic mineral modification still remains to be determined. The results shown in Figure 7 are typical of the types of CL data that were obtained. In this particular study, CL measurements were made on an unprepared sample of silicate rock from the Mojave containing an obvious “green” region with suspected biogenic modification as well as a visibly unaltered area. The CL was obtained from roughly 100 μm-diameter areas within the green region (circled in Fig. 7). As shown in Figure 7 we obtained three different types of CL spectra from the same general region. While the spectral features (peaks at 415 nm and 705 nm) obtained in the green region were different from the 600 nm peak obtained in the unaltered region (not shown), the causes for the observed variations is not known. It is clear that the spatial resolution of our CL measurement was sufficient to distinguish between regions with three unique spectral signatures. Also, the fundamental molecular origin for the 415 nm and 705 nm peaks is as yet undetermined.

Future Development

As evidenced from above, we have barely “scratched the surface” in terms of developing a detailed understanding of the ELXS properties and operating parameters. A big part of the future work will be to focus on developing an in-depth understanding of the CL excitation. First, the specific ionic species responsible for the various CL peaks will be identified. Next, the types of biogenic modification of minerals leading to the generation of CL-active ionic species will be investigated. Finally, the CL activity will be correlated to the XRF-obtained elemental composition, thereby, generating an extensive database of known signatures of life in minerals.

Although electron-beam excited XRF is relatively well understood, in the particular instance of the ELXS, further testing and characterization experiments are necessary in order to develop the system-level specifications for the instrument. These parameters include typical sensor characteristics, such as the signal acquisition times for various kinds of rock and soil samples, accuracy and repeatability in composition determination, sensitivity and dynamic range for the with the laboratory characterization experiments, we are pursuing the development of a scheme to integrate the ELXS on a suitable planetary exploration platform such as a rover (Fig. 8). The ELXS instrument head, consisting of the miniature, encapsulated electron source, high voltage power supply, XRF detector and an optical spectrometer, will be mounted at the end of a deployment “arm” of the rover. The remainder of the instrument system consisting of the control electronics is located within the main body of the rover, within the “Warm Electronics Box”. The key advantage of the ELXS instrument from an overall planetary mission perspective is that no sample manipulation is necessary. Also, the rapid spectrum acquisition capability of the ELXS is expected to enable multiple measurements of targets of interests measurements, and the limits of detection. In parallel during long traverses across the planetary surface.

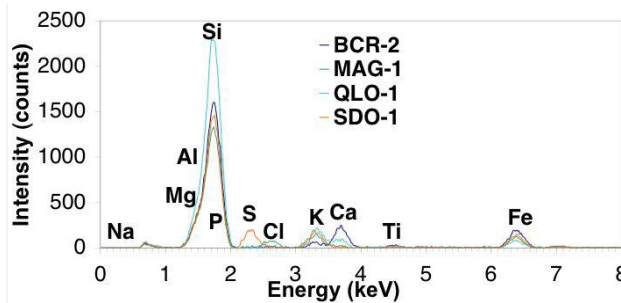


Figure 5. ELXS x-ray fluorescence spectra obtained at Martian environmental pressure from four mineral samples described in the text. Each mineral is easily identified from characteristic peaks present in its respective XRF spectrum. Elemental compositions for elements with atomic number greater than 11 (x-ray detector cutoff) closely match the USGS certified values.

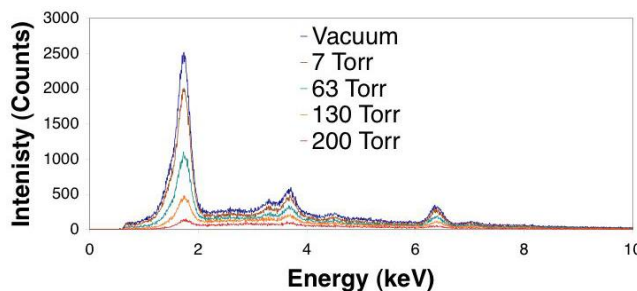


Figure 6. Attenuation of the electron-beam excited XRF signal with increase in ambient pressure. The XRF spectrum was acquired from a Basalt sample. A 7 Torr pressure (Martian ambient) shows negligible attenuation while an ambient pressure over 100 Torr shows significant XRF signal attenuation. The attenuation is more pronounced at lower x-ray energies.

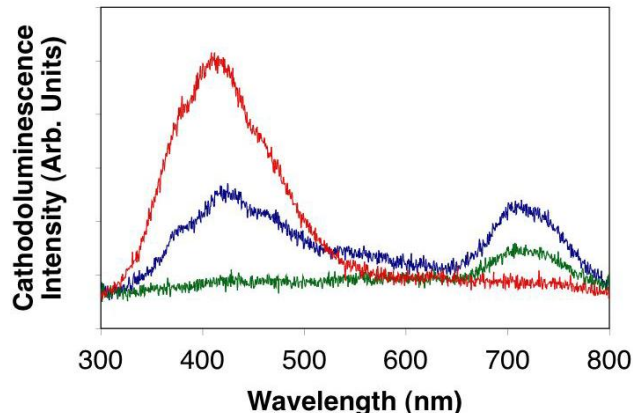


Figure 7. Cathodoluminescence spectra (right) obtained from a green region (circled) on a sample of Mojave silicate rock. The green region is indicative of biogenic activity. However, the cathodoluminescence spectra obtained from roughly 100 μ m-diameter spots within this region exhibit spectral variations as seen in the plot on the right containing three such spectra. In general, two peaks are observed, one at 415 nm and the other at about 705 nm. The origins of these peaks is as yet undetermined.

FORCE-DETECTED NUCLEAR MAGNETIC RESONANCE (FDNMR) SPECTROMETER

Design and Construction

NMR spectroscopy can be conducted using two, very different approaches: the conventional, Faraday-law detection technique and the force-detection technique described below. In both cases, the NMR signal is derived from RF excitation of the sample's nuclear magnetic moment. In the conventional technique, detection occurs by virtue of the induced current in a detector coil generated by the cyclic inversion of the nuclear magnetic moment. FDNMR on the other hand relies on measuring the dipole-dipole force interaction between the sample's nuclear spin magnetic moment and a small detector magnet (of equivalent size to the sample) located in the vicinity of the sample (Fig. 9). The FDNMR spectrometer is constructed using MEMS fabrication techniques.¹⁵ The detector magnet is mounted on a microfabricated Si beam making up a mechanical resonator. The detector magnet sits within an annular magnet (Fig. 9) thus providing a uniform magnetic field over the entire sample volume. RF pulses applied to the sample cyclically invert the nuclear spins of the target isotopes, thereby modulating the dipole-dipole interaction between the detector magnet and the net nuclear magnetic moment of the sample, at the former's mechanical resonance frequency. The resulting motion of the mechanical resonator is detected using a fiber-optic interferometer. The electronics driving the RF coil are capable of producing the desired complex pulse sequences, allowing both single and double resonance NMR experiments. The spectrum acquisition process is described in Figure 10. The displacement of the resonator driven by cyclic inversion of the sample's nuclear magnetic moment is recorded using fiber-optic

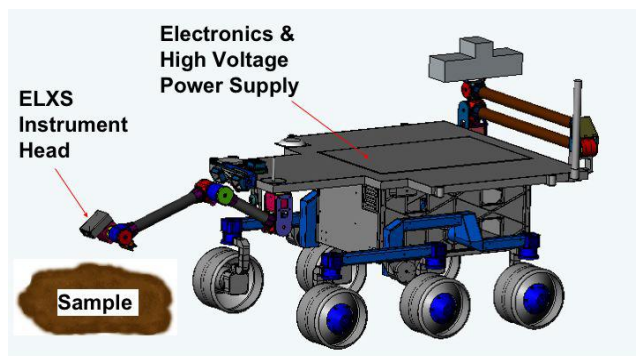


Figure 8. Artist's conception showing the deployment scenario for the ELXS instrument integrated on a planetary exploration rover. The ELXS instrument head is mounted on the rover arm while the control electronics is located within the "Warm Electronics Box" of the rover.

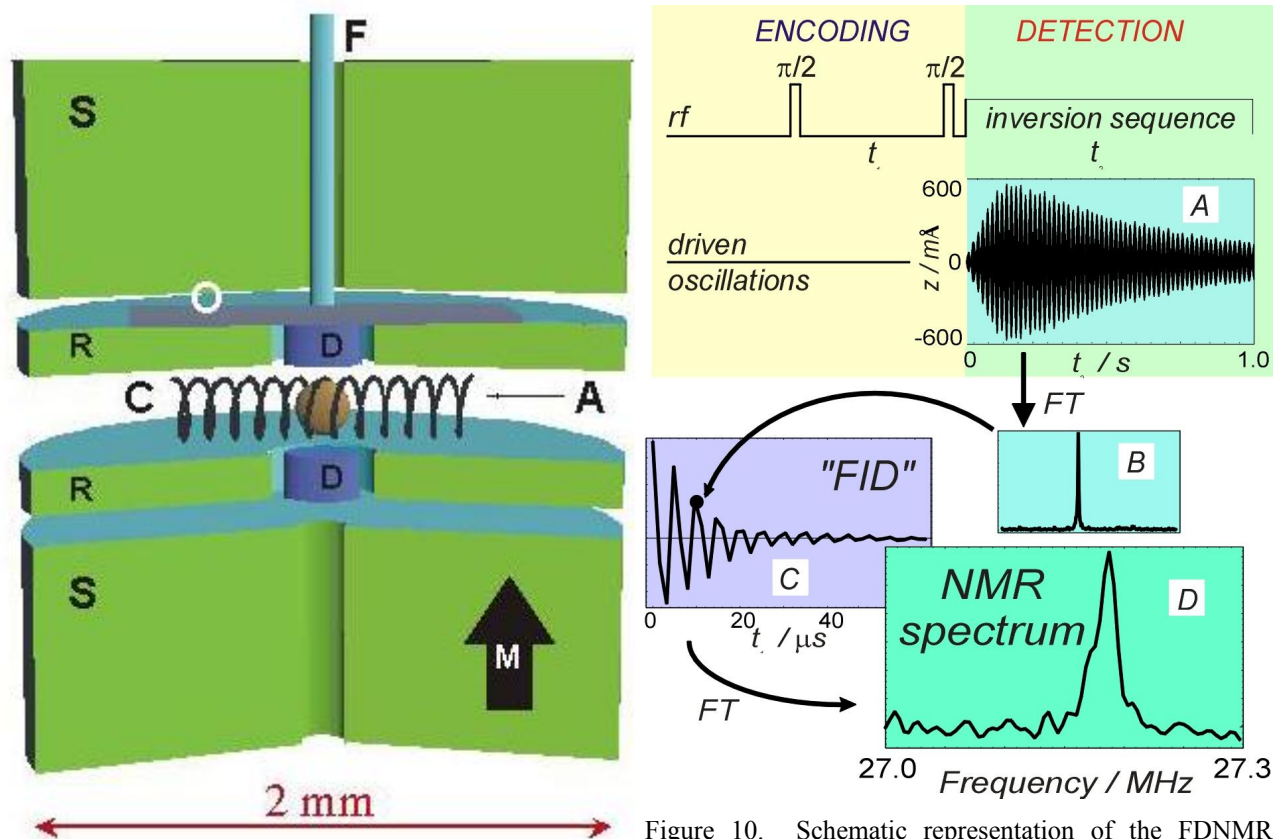


Figure 9. Working principle of the MEMS-based FDNMR spectrometer. The sample (A) sits within an RF excitation coil (C), which modulates the NMR signal at the mechanical resonance frequency of a resonator made up of the detector magnet (D) and silicon beam (O). The detector magnet sits within an annular magnet (R) and the entire assembly is within the pole piece of an external field magnet (S). Detector magnet motion is measured using a fiber optic interferometer (F).

interferometry. A “double” Fourier Transform process is subsequently employed to derive the NMR spectrum from the acquired data. A significant strength of the FDNMR technique over the conventional technique is that it is capable of high-resolution, multi-nuclear analysis.¹⁶ It has been shown previously¹⁵ that the force detection technique is uniquely suited for MEMS sizes and has superior sensitivity over the conventional, inductive detection technique for sample sizes in the range of 10 – 100 microns. Thus, the MEMS FDNMR spectrometer is the only choice for in-line detection of aqueous samples, as well as dissolved organic samples, in a miniaturized, multi-instrument suite type application.

A two-pronged approach was followed in the development of the FDNMR spectrometer. First, a larger sized, mostly conventionally machined, spectrometer was constructed in order to demonstrate the proof-of-principle. The only MEMS component is a Si-beam resonator in this twenty-five-times-the-final-size spectrometer (Fig. 11). As shown in Figure 11,

Figure 10. Schematic representation of the FDNMR spectrum acquisition process. First the sample’s nuclear spin excitation is subjected to an “encoding” process by RF pulses separated by a time t_1 . The mechanical resonator is then driven by cyclic inversion of the sample’s nuclear spin magnetization during the “detection” period t_2 . The mechanical displacement signal A is recorded for a given t_1 value. The Fourier transform (FT) of A yields a spectrum B with a peak at the mechanical resonance frequency. The peak contains phase and amplitude information for a single point in the “FID” (Free Induction Decay) plot C, plotted versus t_1 . In the FDNMR approach, we construct the FID point-by-point unlike in conventional NMR, where it is acquired directly. Next, in both techniques, FT of the FID signal yields the NMR spectrum D. The NMR spectrum shown above represents the first, proof-of-principle proton NMR spectrum from a liquid water sample, acquired by the FDNMR spectrometer at 0.7 Tesla applied field.

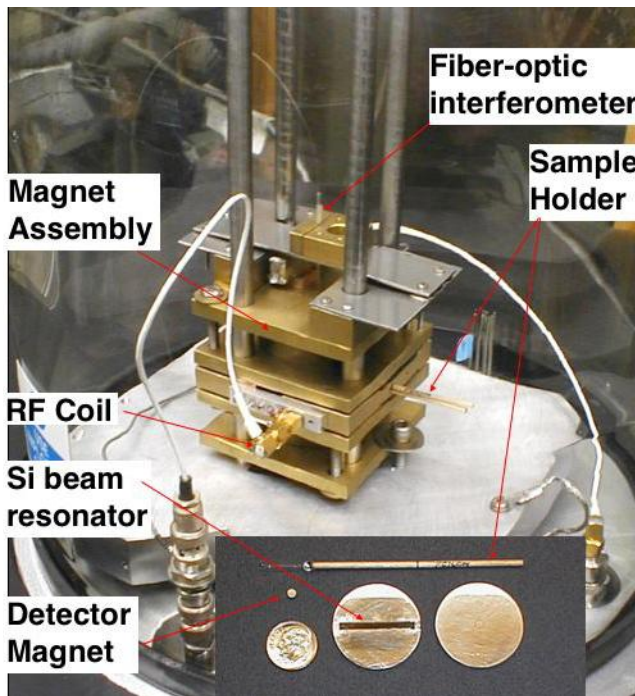


Figure 11. Proof-of-principle apparatus for the FDNMR experiments. The components shown in the inset comprise the FDNMR spectrometer and consist of the detector magnet mounted to a Si beam resonator and placed within an annular magnet. Also shown is the sample holder. The spectrometer is enclosed within the permanent magnet assembly that provides the uniform, 0.7 Tesla field. Also visible are the RF excitation coil and the fiber-optic interferometer. The entire apparatus is placed within an evacuated chamber in order to maximize sensitivity.

the proof-of-principle FDNMR spectrometer consists of a conventionally machined, 2-mm-diameter detector magnet surrounded by a 50 mm annular magnet (shown in the Fig. 11 inset). The Si-beam resonator is bonded to the detector and annular magnets. The entire spectrometer is then mounted within a magnet assembly with an integrated sample holder, RF coil, and a Fabry-Perot fiber-optic interferometer. The proof-of-principle apparatus is placed within an evacuated chamber in order to maximize sensitivity by minimizing atmospheric damping losses for the resonator. The sample is 2.6 mm in diameter.

In parallel with the construction of the proof-of-principle apparatus, the development of the MEMS FDNMR spectrometer was also initiated as shown in Figure 13. Prior to the fabrication and assembly of the MEMS FDNMR spectrometer, four key component technologies needed to be developed. These are:

a. Electroplated, thin-film, soft magnets: In order to achieve as high a resolution as possible for the NMR spectroscopy, it is important that the applied magnetic field be as high as possible. Our research determined that it is possible to electroplate a ternary, soft magnetic alloy of Fe-Ni-Co that is capable of producing a saturated, magnetic field of over 2 Tesla. The challenge lies in developing an electroplating process for a 10- μm -thick film with low stress, good morphology and compositional uniformity. In addition, a precision lithography process was developed to produce thin-walled (1 μm), high aspect ratio (10:1) sacrificial layer “molds” for electroplating the soft magnet film.

b. Si-beam resonator: A novel Deep Reactive Ion Etching process was developed for the fabrication of the Si-beam resonator (Fig. 13) with sufficient mass to counteract the stresses within the plated magnet material and yet have the

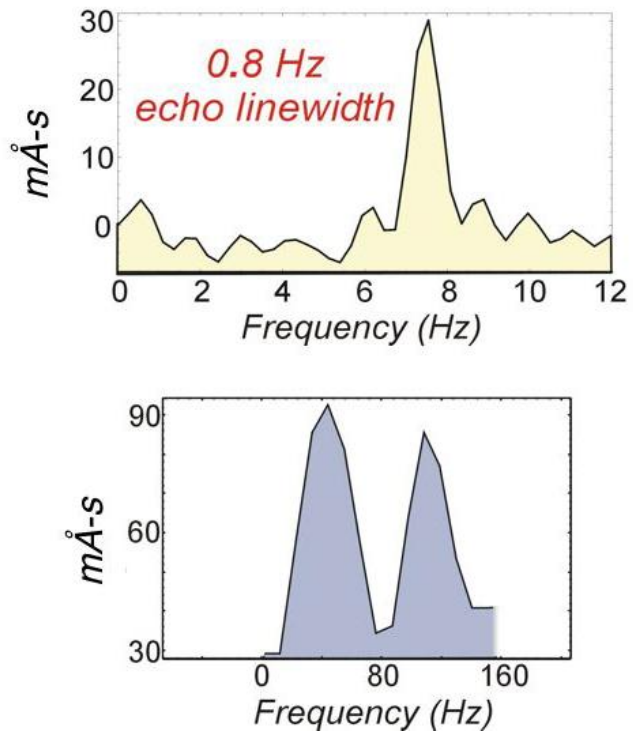


Figure 12. High resolution FDNMR spectra acquired using the proof-of-principle spectrometer. Sophisticated, spin-echo techniques were used to increase the resolution of the NMR spectra. In the upper graph a spectral linewidth of 0.8Hz was obtained for the proton peak in a liquid water sample. In the lower graph, the spectrometer was able to resolve the proton-fluorine J coupling in Acetonitrile (CH_2FCN), at a separation of approximately 80Hz. The ordinate represents the resonator amplitude multiplied by the signal integration time.

long ring down times required for NMR experiments. Following the fabrication of the resonator, a process for releasing the resonator beam without damaging the overlying magnets was also developed.

c. Lateral interferometer: Because of the constrained geometry of the MEMS FDNMR spectrometer, it is not possible to have a vertical, Fabry-Perot geometry as in the case of the proof-of-principle spectrometer. Instead, a novel lateral geometry spectrometer was developed using a beveled end fiber, as shown in Figure 13.

d. Micromachined fixturing for spectrometer assembly: A major challenge in the final assembly of the MEMS spectrometer involves achieving the precise alignment necessary for the various parts of the spectrometer to be put together. In addition, the RF excitation coil and the sample handling system need to be fabricated and co-located within the spectrometer. A novel MEMS-based fixture was designed for the precise assembly of the spectrometer. This fixture is currently in fabrication.

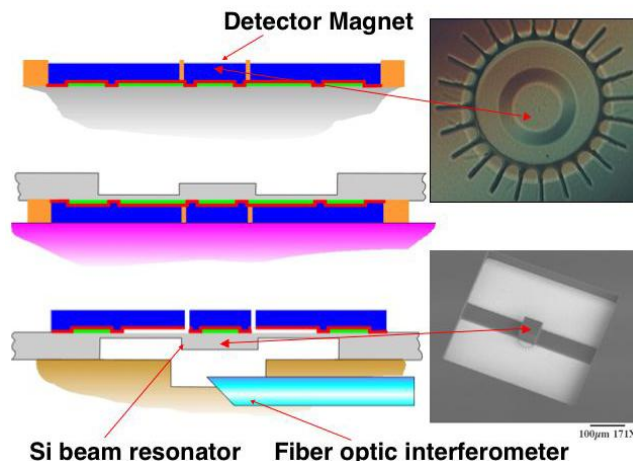


Figure 13, Simplified process schematic showing the major steps for fabrication and assembly of the MEMS FDNMR spectrometer. The steps involve electroplating of a thin-film, multi-component, soft magnet alloy, fabrication of the Si beam resonator and the final assembly of the spectrometer. Shown to the right are an optical micrograph of the electroplated 60 μm detector magnet, and an SEM image of the 400- μm -long Si beam resonator fabricated using Deep Reactive Ion Etching.

Testing and Characterization

The proof-of-principle apparatus shown in Figure 11 was used to acquire the first FDNMR spectrum of protons in water, as shown in Figure 10. This apparatus was also used to demonstrate that it is indeed possible to perform high-resolution NMR experiments at miniaturized size scales by employing sophisticated spin-echo techniques. A record linewidth of 0.8 Hz for proton NMR was achieved using spin-echo pulse sequences (Fig. 12). Also resolved was the proton-fluorine “J” coupling in Acetonitrile, with peaks separated by 80 Hz. Currently, this apparatus is being used to characterize solid mineral samples of astrobiology interest and to develop “finger prints” for each mineral type. One of the first, solid minerals, being studied is gypsum, in order to resolve the characteristic quadruplet proton peaks from the attached water-of-crystallization molecules.

The proof-of-principle apparatus was extremely useful, not only for conclusively demonstrating that high-resolution NMR can indeed be performed at highly-miniaturized scales, but also to develop numerous optimization techniques to enhance the sensitivity and performance of the spectrometer. These included, reduction in the eddy current damping of the resonator due to the motion of the detector, achieving the Brownian noise limit by reducing the noise in the optical interferometer, and achieving long ring-down times (~ 1 s) by reducing attachment loss for the beam resonator. In parallel with the experimental work, computer simulations of spectrometer behavior were developed and refined based on the experimental results. In regard to the MEMS-scale spectrometer, as described above, the testing was performed mainly at the sub-component level to ensure the reliability and performance of each of the thin-film magnet, Si beam resonator and the lateral beam interferometer.

Future Development

The MEMS FDNMR spectrometer technology is at a lower maturity level in comparison to the ELXS technology. However, it promises to augment the NASA instrument “toolset” with an exciting new astrobiology capability. Following the assembly, integration and demonstration of the MEMS FDNMR spectrometer, we will initiate the development of the instrument sub-system. As a first step to the sub-system development we plan to design and integrate a microfluidic, sample transport system that can controllably locate the sample with the FDNMR spectrometer. First, the sample will be placed under the 2 mm annular magnet, during the “encoding” phase. Next, the sample will be located under the detector magnet for the NMR signal acquisition. Ultimately, we hope to integrate the MEMS FDNMR spectrometer subsystem within a multi-instrument suite for in-situ planetary astrobiology exploration.

TECHNOLOGY TRANSITION

Infusion of new instrument technologies into NASA missions is a long and tedious process. Newly developed technologies have to demonstrate sufficient “maturity” as defined by NASA’s Technology Readiness Level (TRL) scale.¹⁸ The TRL scale ranges from levels 1 through 9, from basic research into demonstrating the proof-of-concept (TRL 1-3), to reliable demonstration of subsystems based on the new technologies (TRL 4-6), and finally, to successful utilization of these subsystems in NASA’s space missions (TRL 7-9). The maturity of the ELXS is assessed to be around TRL 3 while the FDNMR spectrometer is at TRL 2. The next step for these technologies is to demonstrate reliable performance at the sub-system level in the laboratory environment, followed by a demonstration in a “relevant,” space-like environment. These demonstrations typically require an order of magnitude increase in effort and funding. NASA’s Mars Technology Program is set up to help new, Mars-relevant technologies bridge this infamous mid-TRL “Valley of Death”. Also, commercial development of these technologies can be pursued as an alternative maturation path. The ultimate “customer” in the NASA world is the planetary astrobiology scientist, who proposes the instrument for a future in-situ landed mission.

ACKNOWLEDGEMENTS

The research described in this paper was carried out at the Jet Propulsion Laboratory, California Institute of Technology, under a contract with the National Aeronautics and Space Administration.

REFERENCES

1. Details of the first Explorer mission can be found at: <http://www.hq.nasa.gov/office/pao/History/explorer.html>
2. D. Morrison and G.K. Schmidt, Editors *Astrobiology Roadmap*, <http://astrobiology.arc.nasa.gov/roadmap/>, NASA Ames Research Center, Moffett Field, CA (1999).
3. K. Biemann, J. Oro, P. Toulmin, L.E. Orgel, A.O. Nier, D.M. Anderson, P.G. Simmonds, D. Flory, A.V. Diaz, D.R. Rushneck, J.E. Biller, and A.L. Lafleur, “The Search for Organic Substances and Inorganic Volatile Compounds in the Surface of Mars.” *J. Geo. Res.* 82, 4641-4658 (1977).
4. E.A. Flinn, “Scientific Results of the Viking Project”, *J. Geo. Res.* 82, 735 (1977).
5. J.M. Jenkins, P. G. Steffes, D.P. Hinson, J.D. Twicken, and G.L. Tyler, “Radio Occultation Studies of the Venus Atmosphere with the Magellan Spacecraft”, *Icarus* 110, 79-94, (1994).
6. Facts on Jupiter’s icy moon Europa can be found at: <http://www.johnstonsarchive.net/astro/europa.html>
7. A. Tripathi and J. Zachos, “Late Eocene tropical sea surface temperatures: A perspective from Panama”, *Paleoceanography* 17, 4.1 (2002).
8. T. George, “Miniature Electron Microscopes without Vacuum Pumps”, *NASA Tech Briefs*, NPO-20335, Aug. 1998.
9. J.Z. Wilcox, E. Urgiles, S. Douglas and T. George, “Electron-induced Luminescence and X-ray Spectrometer Development: Progress Report”, *IEEE Aero. Conf. Proc.* 2, 569 (2003).
10. E. D. Green and G. S. Kino, *J. Vac. Sci. Tech.* B9, 1557 (1991).
11. G. D. Danilatos, *Scanning* 7, 1 (1985); *Scanning Microscopy* 4, 799 (1999).
12. R. Reider, H. Wanke, T. Economou, and J. Turkevich, *J. Geo. Res.* E2, 102 (1997).
13. The APXS flew on the Mars Exploration Rover missions. Details at: <http://www.planetary.org/mars/mer-inst-apxs.html>. The APXS also flew on the Mars Pathfinder mission. Details at: M. P. Golombek, R. A. Cook, T. Economou, W. M. Folkner, A. F. C. Haldemann, P. H. Kallemeyn, J. M. Knudsen, R. M. Manning, H. J. Moore, T. J. Parker, R. Rieder, J. T. Schofield, P. H. Smith, and R. M. Vaughan, “Overview of the Mars Pathfinder Mission and Assessment of Landing Site Predictions”, *Science* 278, 1743-1748 (1997).
14. J.R. Marshall, L. Koppel, C. Bratton, E. Metzger, and M. Hecht, “A combined XRD-XRF-optical hands on instrument for analysis of cometary-surface material,” private communication (1997).
15. T. George, L.A. Madsen, W. Tang, A. Chang-Chien, G.M. Leskowitz, and D.P. Weitekamp, “MEMS-based force-detected nuclear magnetic resonance spectrometer for *in situ* planetary exploration”, *Aero. Conf. IEEE Proc.* 1, 273-278 (2001).
16. G.M. Leskowitz, L.A. Madsen, and D.P. Weitekamp, “Force-detected magnetic resonance without field gradients”, *Sol. St. Nucl. Magn. Reson.* 11, 73-86, 1998.
17. E. Urgiles, J.Z. Wilcox, R. Toda, J. Crisp, and T. George, “Atmospheric Electron-Induced X-Ray Spectrometer (AEXS) Instrument Development,” 36th Lunar and Planetary Science Conference, League City Texas, March 14-18 2005.
18. For info on NASA’s Technology Readiness Level (TRL) Scale: <http://www.hq.nasa.gov/office/codeq/trl/index.htm>